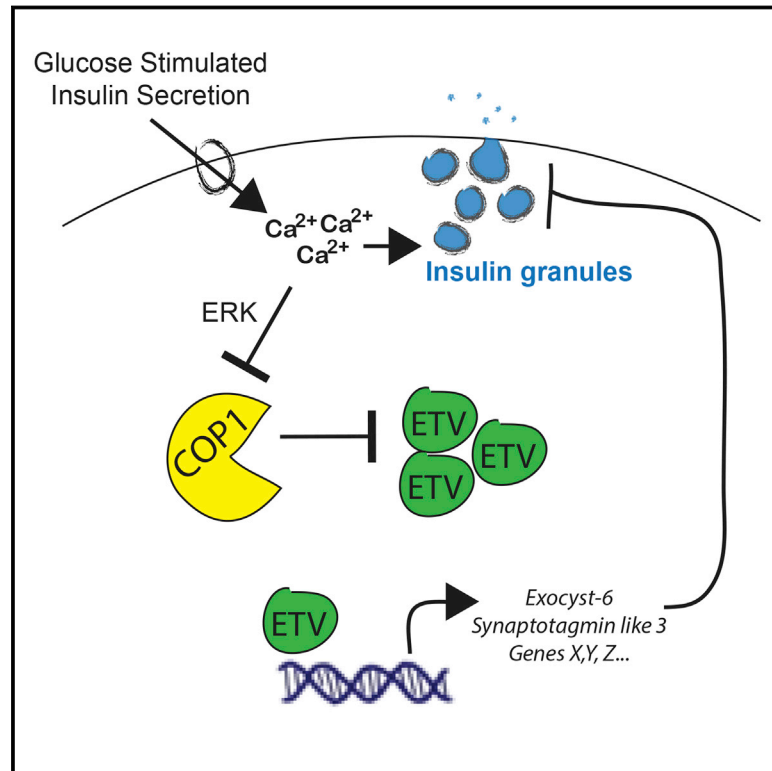# β-Cell Insulin Secretion Requires the Ubiquitin Ligase COP1

Graphical Abstract

Authors

Rowena Suriben, Kelly A. Kaihara, Magdalena Paolino, ..., Jinfeng Liu, Matthias Hebrok, Vishva M. Dixit

Correspondence

dixit@gene.com

In Brief

In adult pancreatic β cells, the post-translational regulation of the transcription factors ETV1, ETV4, and ETV5 by the ubiquitin ligase COP1 is critical for insulin secretion and the maintenance of normal glucose homeostasis. Dysregulation of this axis leads to the mis-expression of several ETV-target genes that are linked to diabetes and obesity.

Highlights

- Loss of COP1 in β cells caused insulin secretion defects and hyperglycemia

- Deletion of transcription factors ETV1, ETV4, and ETV5 rescued COP1 phenotypes

- ETV-dependent genes were significantly enriched in human diabetes and obesity GWAS

- ETV transcription factors limited insulin secretion under hyperglycemic conditions

Accession Numbers

GSE70788

CellPress

Article

β-Cell Insulin Secretion Requires the Ubiquitin Ligase COP1

Rowena Suriben,[1] Kelly A. Kaihara,[2] Magdalena Paolino,[1] Mike Reichelt,[3] Sarah K. Kummerfeld,[4] Zora Modrusan,[5] Debra L. Dugger,[1] Kim Newton,[1] Meredith Sagolla,[3] Joshua D. Webster,[3] Jinfeng Liu,[4] Matthias Hebrok,[2] and Vishva M. Dixit[1],*

[1]Department of Physiological Chemistry, Genentech, 1 DNA Way, South San Francisco, CA 94080, USA
[2]Diabetes Center, University of California, San Francisco, San Francisco, CA 94143 USA
[3]Department of Pathology
[4]Department of Bioinformatics and Computational Biology
[5]Department of Molecular Biology
Genentech, 1 DNA Way, South San Francisco, CA 94080, USA
*Correspondence: dixit@gene.com
http://dx.doi.org/10.1016/j.cell.2015.10.076

SUMMARY

A variety of signals finely tune insulin secretion by pancreatic β cells to prevent both hyper-and hypo-glycemic states. Here, we show that post-transla-tional regulation of the transcription factors ETV1, ETV4, and ETV5 by the ubiquitin ligase COP1 (also called RFWD2) in β cells is critical for insulin secre-tion. Mice lacking COP1 in β cells developed dia-betes due to insulin granule docking defects that were fully rescued by genetic deletion of *Etv1, Etv4*, and *Etv5*. Genes regulated by ETV1, ETV4, or ETV5 in the absence of mouse COP1 were enriched in hu-man diabetes-associated genes, suggesting that they also influence human β-cell pathophysiology. In normal β cells, ETV4 was stabilized upon mem-brane depolarization and limited insulin secretion un-der hyperglycemic conditions. Collectively, our data reveal that ETVs negatively regulate insulin secretion for the maintenance of normoglycemia.

INTRODUCTION

Inadequate insulin release in response to glucose is a hallmark in the progression of type 2 diabetes. Initially thought of as a dis-ease primarily driven by insulin resistance, it is now clear that β-cell dysfunction and impaired insulin release are key contribu-tors to the chronic hyperglycemia seen in type 2 diabetic patients (Kahn, 1998, 2001; Weir and Bonner-Weir, 2004). Secreted from pancreatic β cells in response to elevated glucose load, insulin is the sole hormone able to reduce blood glucose levels (Rorsman and Braun, 2013). While β cells activate a number of mechanisms to increase insulin secretion in response to elevated glucose (Prentki and Nolan, 2006), sus-tained hyperglycemia or hyperkalemia elicits a dose-dependent decrement in β-cell insulin secretion (Eizirik et al., 1992; Yama-zaki et al., 2006). Termed β-cell desensitization, this decrease in insulin secretion correlates with degranulation of the β cell and can be reversed upon removal of the stimulant (Rustenbeck

et al., 2004). Nonetheless, in patients with type 2 diabetes, the long-term hyperglycemic environment imposes irreversible β-cell damage (glucose toxicity) that cannot be overcome without medical intervention.

The ubiquitin ligase COP1 was initially identified in plants as an essential negative regulator of light-mediated plant develop-ment (Lau and Deng, 2012). Thus, when plants are grown in the dark, COP1 represses photomorphogenesis by ubiquitylating bZIP transcription factors driving the photomorphogenic pro-gram and this targets them for proteasomal degradation. Following exposure to light, COP1 activity is excluded from the nucleus and its transcription factor substrates are stabilized, allowing for the transcription of light-inducible genes. Remark-ably, a majority of all light-controlled genes, representing greater than 20% of the plant genome, are influenced by COP1 (Ma et al., 2002).

COP1 also exists in a multi-subunit ubiquitin ligase in mam-mals. Reported substrates include c-JUN, ETV1, c/EBPα, acetyl-coenzyme A carboxylase, and CREB-regulated tran-scription co-activator 2 (CRTC2) (Dentin et al., 2007; Marine, 2012; Qi et al., 2006). Studies of COP1-deficient mice indicated a role for COP1 in tumor suppression (Vitari et al., 2011; Miglior-ini et al., 2011). For example, COP1 deletion in prostate epithe-lium stabilized the transcription factors cJUN, ETV1, and ETV4 and led to the development of prostate intraepithelial neoplasia (Vitari et al., 2011). ETV1, ETV4, and ETV5 belong to the Pea3 group of the ETS family of transcription factors. Activated down-stream of receptor tyrosine kinases, Pea3 transcription factors regulate cell-type specific gene programs involved in cell differ-entiation, signaling, and tissue morphogenesis (Lu et al., 2009; Mao et al., 2009; Zhang et al., 2009). A recent study of ETV5-deficient mice implicated ETV5 in glucose metabolism (Gutier-rez-Aguilar et al., 2014). Interestingly, genome-wide association studies (GWASs) have linked ETV5 and obesity (Welter et al., 2014).

Here we identify a function for COP1 in regulating β-cell insulin secretion. Deletion of COP1 from adult mouse β cells caused the accumulation of Pea3 transcription factors and this activated genes inhibitory to insulin secretion. β-cell defects associated with COP1 loss could be ameliorated by the deletion of ETV1, ETV4, and ETV5. Identification of the β-cell genes regulated by
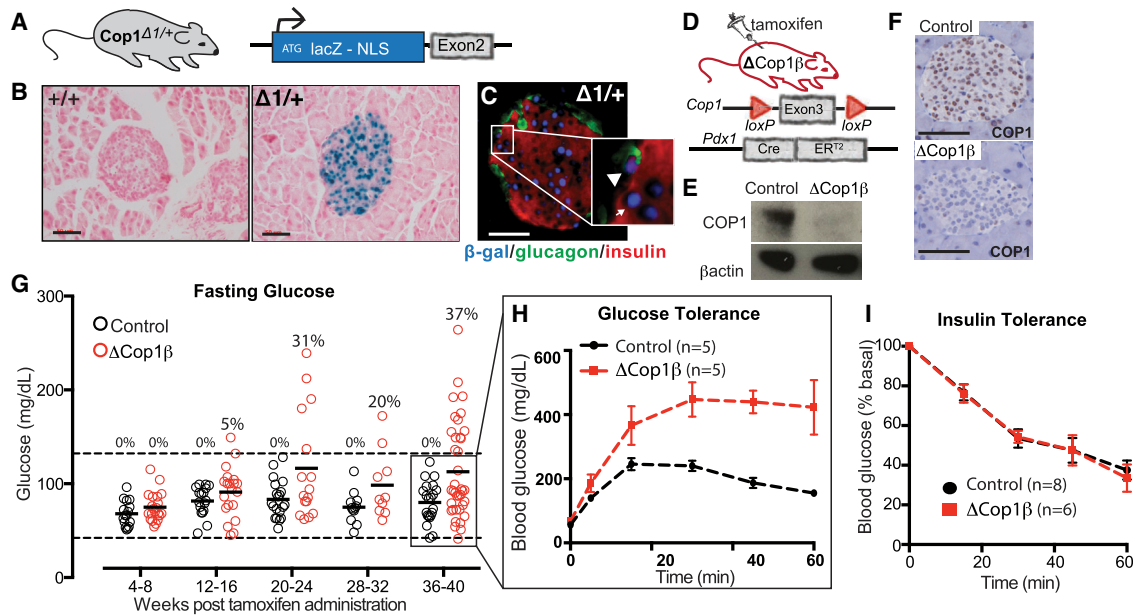
Figure 1. Loss of COP1 in Adult β Cells Promotes Hyperglycemia in Mice

(A) Schematic shows the $Cop1^{\Delta 1/+}$ allele with a *lacZ* reporter gene. NLS, nuclear localization sequence.

(B) Detection of β-galactosidase enzymatic activity (blue) in $Cop1^{+/+}$ and $Cop1^{\Delta 1/+}$ adult pancreas is shown. Black bar, 50 μm.

(C) Detection of β-galactosidase enzymatic activity (blue) and immunofluorescence staining of insulin (red, arrow) and glucagon (green, arrowhead) in a $Cop1^{\Delta 1/+}$ islet are shown. White bar, 50 μm.

(D) Schematic for *Cop1* deletion in β cells (ΔCop1β). $Cop1^{fl/fl}$ Pdx1.CreERT2 mice were dosed at 8 weeks of age.

(E) Immunoblot for COP1 in control (Pdx1.CreERT2) and ΔCop1β islets is shown.

(F) COP1 protein expression in control and ΔCop1β islets was detected by immunohistochemistry. Black bar, 50 μm.

(G) Fasting blood glucose levels. Each symbol represents one mouse. Black line indicates the mean. Dashed lines mark 60 and 120 mg/dl.

(H) Intraperitoneal glucose tolerance tests (GTTs) of normoglycemic mice at 36 weeks post-tamoxifen are shown.

(I) Insulin tolerance tests of hyperglycemic ΔCop1β and control mice are shown.

Data are represented as mean ± SEM (*p < 0.05, **p < 0.005, and ***p < 0.0005 by unpaired Student's t test). Analyses in (E) and (F) used mice at 3 weeks post-tamoxifen. See also Figure S1.

ETV1, ETV4, and ETV5 revealed a significant enrichment of diabetes and obesity-associated genes and included genes involved in insulin granule docking. In normal β cells, ETV4 was stabilized upon membrane depolarization and limited insulin release under hyperglycemic conditions. Therefore, this study identifies a requirement for COP1 and ETV transcription factors in β-cell insulin secretion, and it illuminates an inhibitory mechanism that can be activated in situations of increased secretory demand.
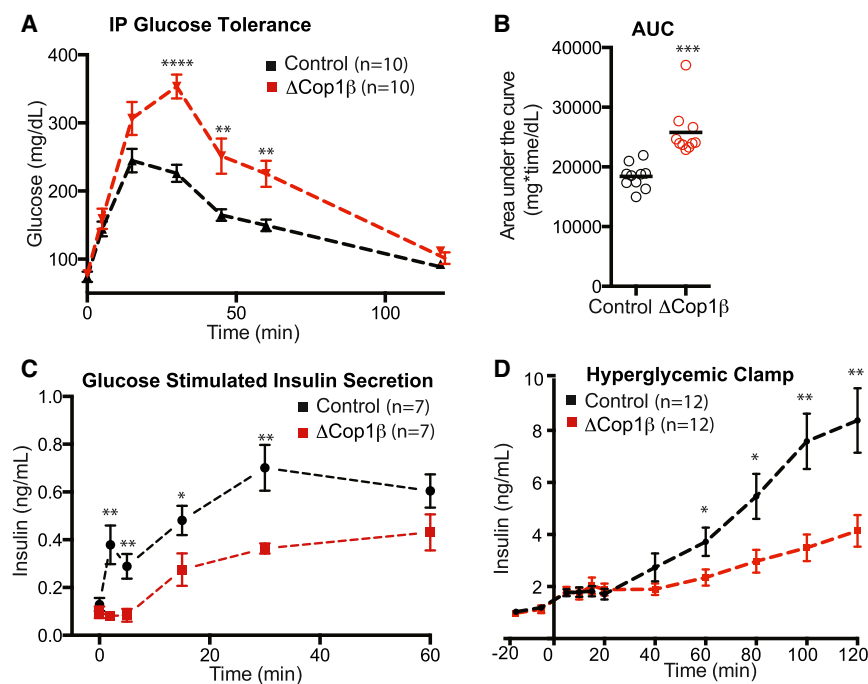
RESULTS

Deletion of COP1 in Adult β Cells Causes Hyperglycemia in Mice

$Cop1^{\Delta 1/+}$ mice (Vitari et al., 2011) with a *lacZ* reporter gene replacing exon 1 of one *Cop1* allele (Figure 1A) revealed *Cop1* to be highly expressed in adult pancreatic islets (Figure 1B). β-galactosidase activity was detected in both insulin-producing β cells and glucagon-producing α cells (Figure 1C). To determine the role of COP1 in adult β cells, mice bearing conditional alleles of *Cop1* ($Cop1^{fl/fl}$) (Vitari et al., 2011) and a Pdx1.CreERT2 transgene (Gu et al., 2002) were dosed with tamoxifen at 8 weeks of age to inactivate *Cop1* in adult β cells

(hereafter referred to as ΔCop1β mice, Figure 1D). Three weeks after dosing, islets from ΔCop1β mice contained markedly less COP1 protein than islets from $Cop1^{+/+}$ Pdx1.CreERT2^{+} control mice (Figures 1E and 1F). Importantly, no recombination was detected in the brain (Figure S1A) as has been reported for some loci using *Pdx1* drivers (Magnuson and Osipovich, 2013).

Blood glucose levels in ΔCop1β mice fasted for 15–18 hr remained within the normal range of 60–120 mg/dl for up to 8 weeks following tamoxifen treatment, but thereafter fasted and randomly fed blood glucose levels were elevated in a subset of the mice (Figure 1G; Figure S1B). After 36–40 weeks, 37% of ΔCop1β mice had elevated glucose levels compared to 0% of controls (Figure 1G). ΔCop1β animals that remained normoglycemic were severely glucose intolerant (Figure 1H). Glycemic variability in ΔCop1β animals was not due to differences in $Cop1^{fl/fl}$ recombination because normoglycemic ΔCop1β mice had comparable levels of COP1 compared to hyperglycemic animals (Figures S1C and S1D). Further, body weights of ΔCOP1β mice after 36 weeks were comparable to those of controls (Figure S1E) and they exhibited normal insulin tolerance (Figure 1I), thereby ruling out insulin insensitivity as a cause of hyperglycemia in ΔCOP1β animals.

A   IP Glucose Tolerance

B   AUC

C   Glucose Stimulated Insulin Secretion

D   Hyperglycemic Clamp

Figure 2. Deletion of COP1 Results in Glucose Intolerance and Decreased Insulin Secretion

(A) Intraperitoneal GTTs are shown.

(B) Quantification of area under the curve (AUC) for individual GTTs. Black line indicates the mean.

(C) In vivo glucose-stimulated insulin secretion (GSIS) is shown.

(D) Plasma insulin levels upon hyperglycemic clamping are shown.

Data are represented as mean ± SEM (*p < 0.05, **p < 0.005, and ***p < 0.0005 by unpaired Student's t test). Analyses used mice at 3 weeks post-tamoxifen with fasting blood glucose levels between 60 and 120 mg/dl. See also Figures S2, S3, and S4.

COP1 Is Required for Glucose-Stimulated Insulin Secretion

Given that the hyperglycemia seen in ΔCop1β mice was not due to insulin insensitivity, we looked for defects in β-cell function and/or maintenance. ΔCop1β mice exhibited defects in glucose clearance as early as 3 weeks after tamoxifen treatment as measured by intraperitoneal and oral glucose tolerance tests (GTTs) (Figures 2A and 2B; Figure S2A). Importantly, glucose intolerance was not seen in Cop1$^{fl/fl}$ Pdx1.CreERT2$^+$ mice not treated with tamoxifen (Figure S2B). The inability of ΔCop1β mice to clear blood glucose as efficiently as controls was a consequence of decreased glucose-stimulated insulin secretion (GSIS; Figure 2C). Whereas control animals exhibited an initial burst of insulin secretion within 5 min of glucose challenge (the expected first-phase response) followed by a more sustained period of insulin secretion (the second-phase response), ΔCop1β mice lacked a first-phase response and their second-phase response was attenuated. ΔCop1β mice also exhibited defective insulin secretion after blood glucose levels were clamped at 250 mg/dl (Figures S2C–S2E). Basal plasma insulin levels did not differ between ΔCop1β and control mice, but, upon glucose infusion, control animals showed a 4-fold increase in plasma insulin whereas ΔCop1β animals averaged less than a 2-fold increase (Figure 2D).

Decreased insulin secretion could reflect changes in β-cell mass, differentiation state, and/or defects in insulin production or processing (Kitamura, 2013; Orci et al., 1985; Talchai et al., 2012). The ΔCop1β pancreas contained normal numbers of islets that resembled control islets in terms of their size and expression of genes associated with mature β cells (Figures S3A–S3L). The amount of insulin and its cellular distribution in ΔCOP1β islets was also equivalent to that seen in control islets (Figures S4A–S4G). These observations suggested that COP1 deficiency might impact GSIS directly.

COP1 Deletion Results in Impaired Insulin Granule Docking and Exocytosis

β-cell GSIS is activated following the Glut2-dependent import of glucose, whereupon it is metabolized and intracellular ATP is increased. K$_{ATP}$ channel closure causes membrane depolarization and induces Ca^{2+} influx, which ultimately activates insulin secretory vesicles for release (Rorsman and Braun, 2013; Figure 3A). The absence of first-phase insulin secretion in ΔCop1β mice (Figure 2C) suggested a failure to release the pre-formed insulin granules that are located close to the plasma membrane (Seino et al., 2011). Consistent with this notion, the membrane-depolarizing agents KCl and arginine triggered significantly less insulin secretion from ΔCop1β islets than from control islets (Figure 3B). Islet perifusion to measure dynamic insulin secretion (Figure 3C) corroborated this defect because ΔCop1β islets released very little insulin when exposed to high glucose or KCl compared to controls (Figure 3D). Ca^{2+} influx subsequent to membrane depolarization was normal in ΔCop1β islets (Figure 3E), suggesting that the secretion defect might be due to a problem with the insulin granules themselves.

We tested if the failure to release pre-formed insulin granules (the first-phase response) in ΔCop1β islets could be ameliorated with the incretin mimetic and GSIS agonist Exendin-4 (Drucker and Nauck, 2006). Activation of incretin receptors GIP and GLP-1 increases cAMP, which activates both PKA-dependent and -independent mechanisms to prime insulin vesicles for release (Seino and Shibasaki, 2005; Seino et al., 2011; Song et al., 2011). This priming step potentiates the first phase of insulin secretion in response to glucose. As expected, Exendin-4 pretreatment (Figure 3F) enhanced GSIS in control animals (Figure 3G) and improved glucose tolerance (Figure 3H). The ΔCOP1β mice also responded to Exendin-4 with increased GSIS (Figure 3G) and this normalized glucose tolerance to control levels (Figure 3H; compare red and black solid lines). Direct activation of either PKA or the guanine nucleotide exchange factor Epac, components downstream of incretin signaling, also potentiated insulin exocytosis in
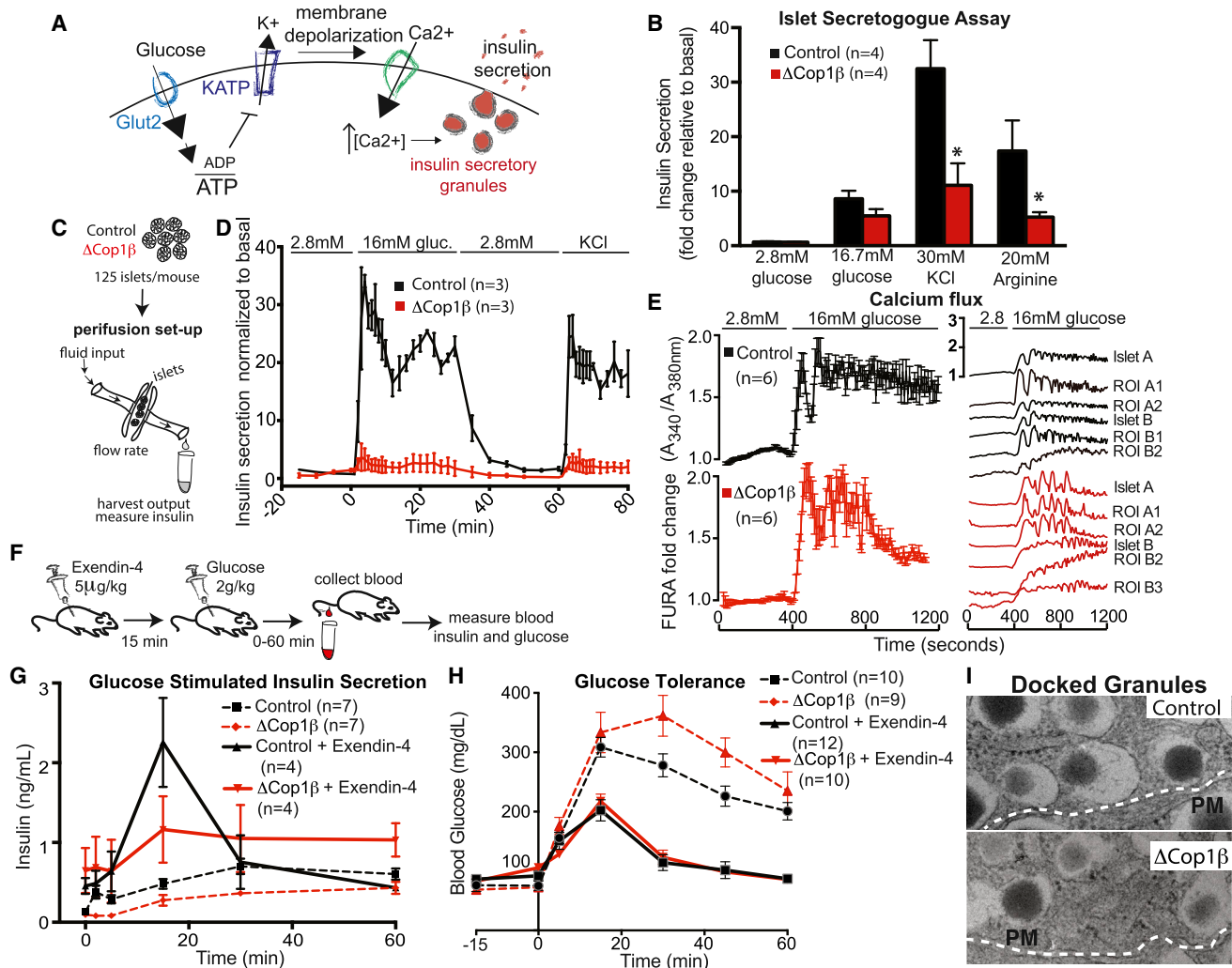
Figure 3. COP1 Functions in GSIS

(A) Schematic shows GSIS.

(B) Insulin secretion from islets incubated in vitro with the stimuli indicated for 1 hr at 37°C is shown.

(C) Schematic of islet perifusion setup as previously described (Kaihara et al., 2013). Islets (125 per animal) were perifused with various secretogogues: basal glucose (2.8 mM), high glucose (16.6 mM), or 30 mM KCl.

(D) Dynamic insulin secretion of islets in the perifusion chamber is shown. Error bars, SEM.

(E) Fura-2 imaging of calcium flux in islets is shown. ROI, region of interest.

Data are represented as mean ± SEM (*p < 0.05 by unpaired Student's t test). Analyses used mice at 3 weeks post-tamoxifen.

(F) Schematic shows Exendin-4 treatment prior to GSIS assay.

(G) Intraperitoneal GTTs are shown.

(H) In vivo GSIS.

(I) Electron micrographs of β cells. White dotted line outlines plasma membrane. Scale bars, 0.2 μm.

Analyses used mice at 3 weeks post-tamoxifen with fasting blood glucose levels between 60 and 120 mg/dl. See also Figure S5.

ΔCop1β islets (Figure S5A). These data indicate that ΔCop1β insulin granules can be released if the exocytosis defect caused by COP1 deficiency is bypassed by activation of the incretin pathway.

The first-phase insulin response releases insulin granules already docked at the plasma membrane (Rorsman and Renström, 2003). To determine if ΔCop1 β cells had fewer docked granules, we performed morphometric analyses on electron micrographs of islets. In comparison to control β cells, ΔCOP1 β cells had fewer docked granules, defined as having cores between 0 and 100 nm from the plasma membrane (Figures 3I, 5B, and 5C). These results, along with the finding that first-phase insulin secretion is absent in ΔCOP1β animals, are consistent with a function for COP1 in the docking of insulin secretory granules necessary for glucose-stimulated release.
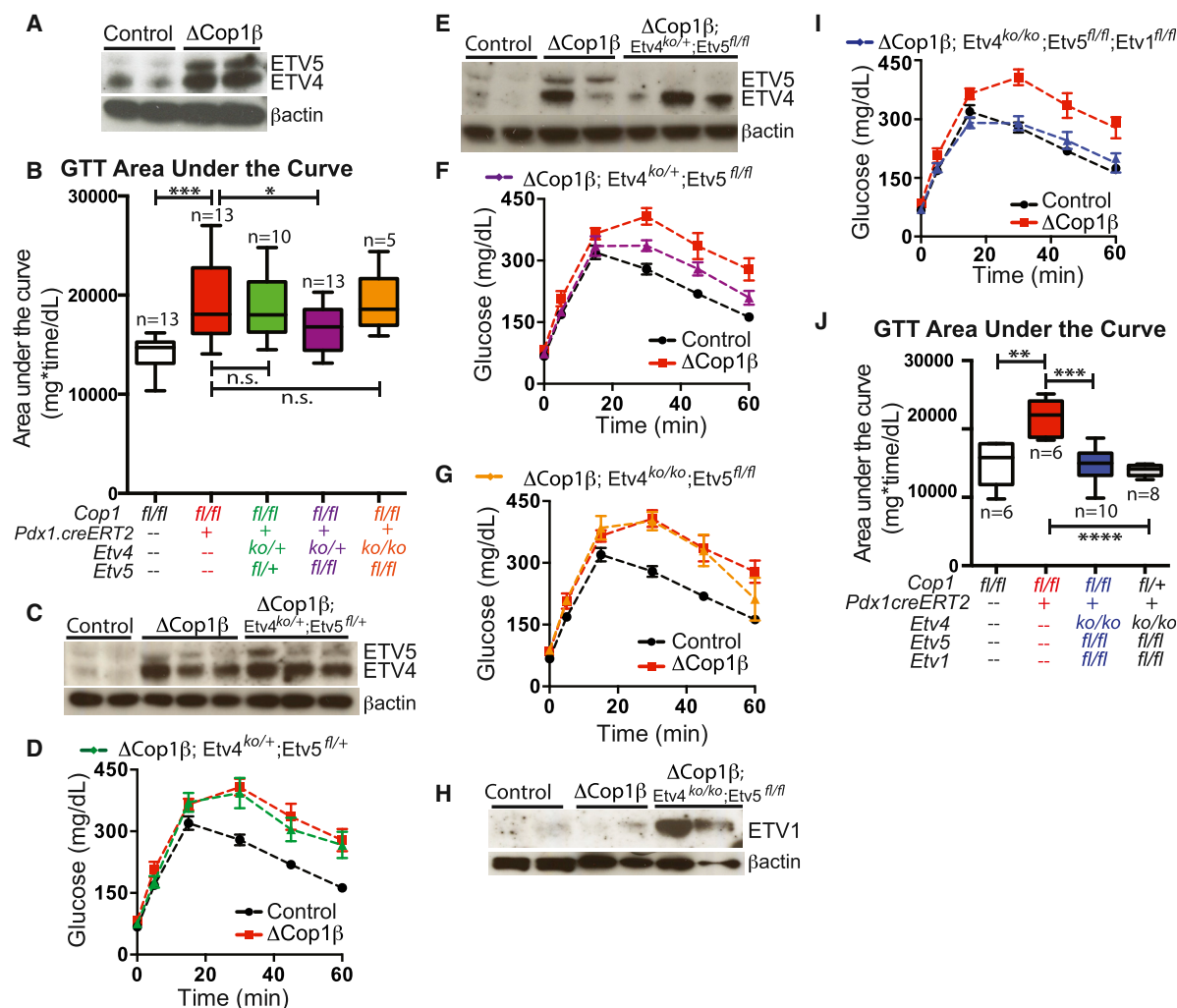
Figure 4. ETV Transcription Factors Are the Critical Substrates for COP1 in β Cells

(A, C, E, and H) Immunoblots of ETV1, ETV4, and ETV5 in islets are shown.

(B and J) Intraperitoneal GTT AUC was calculated for each individual animal and grouped by genotype.

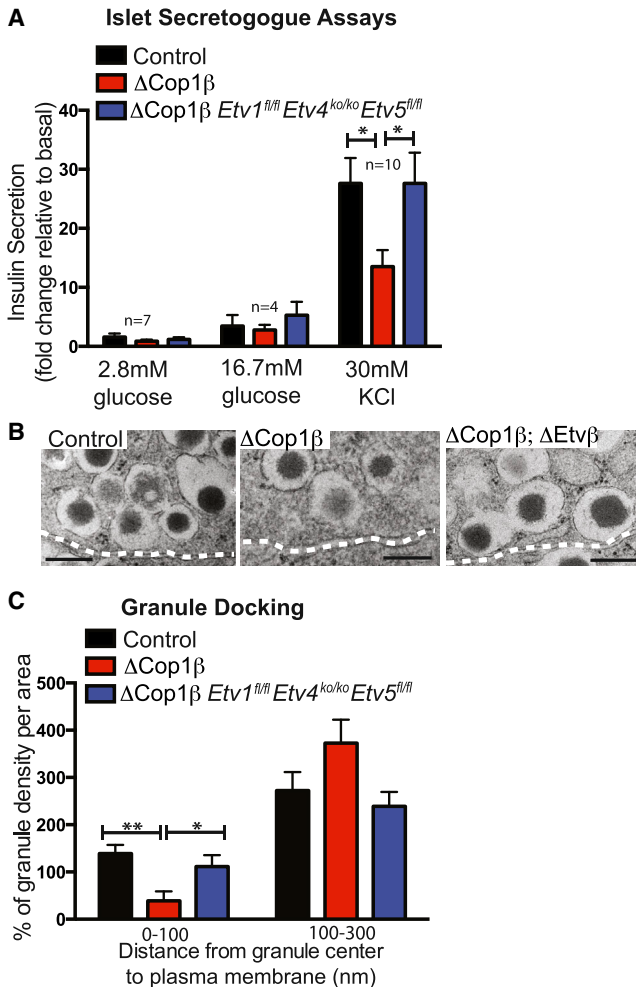(D, F, G, and I) GTTs on the genotypes indicated are shown.

For AUC box and whisker graphs, error bars indicate the range. Box represents 25th–75th percentile with line at median value (*p < 0.05, **p < 0.005, ***p < 0.0005, and ****p < 0.00005 by unpaired Student's t test). Analyses used mice at 3 weeks post-tamoxifen with fasting blood glucose levels between 60 and 120 mg/dl. See also Figure S6.

Pea3 Transcription Factors Are the Critical COP1 Substrates in Pancreatic β Cells

To better understand the insulin secretion defect in ΔCop1β mice, we determined the critical substrates of COP1 in β cells. Several proteins are ubiquitylated and targeted for proteasomal degradation by COP1 (Marine, 2012), including ETV1, ETV4, and ETV5. ETV4 and ETV5 proteins (Figure 4A), but not mRNAs (Figures S6A and S6B), were more abundant in ΔCop1β islets than in control islets, which is consistent with post-transcriptional regulation of ETV4 and ETV5 by COP1 in β cells. ETV1, however, was not elevated significantly in ΔCop1β islets (Figure 4H). We tested whether increased ETV4 and ETV5 were responsible for the insulin secretion defect in ΔCop1β mice by introducing $Etv4^{ko}$ mutant and/or conditional $Etv5^{fl}$ alleles

(Zhang et al., 2009). The mutant $Etv4$ and $Etv5$ alleles were on a mixed genetic background, which itself did not alter the glucose intolerance of the ΔCop1β mice (Figure 4B, compare white versus red bars), which originally had an inbred C57BL/6 background (Figure 2A).

The ΔCop1β $Etv4^{ko/+}$ $Etv5^{fl/+}$ mice still expressed more ETV4 and ETV5 proteins in their islets than control mice (Figure 4C) and were glucose intolerant (Figures 4B and 4D), but ΔCop1β $Etv4^{ko/+}$ $Etv5^{fl/fl}$ mice showed less severe glucose intolerance than ΔCop1β mice (Figures 4B, 4E, and 4F). Elimination of the remaining $Etv4$ wild-type allele did not further ameliorate the glucose intolerance. Indeed, ΔCop1β $Etv4^{ko/ko}$ $Etv5^{fl/fl}$ mice were indistinguishable from ΔCop1β mice (Figures 4B and 4G). Immunoblotting revealed that ETV1 was abnormally high in

A **Islet Secretogogue Assays**

Legend:
- Control
- ΔCop1β
- ΔCop1β *Etv1*^fl/fl *Etv4*^ko/ko *Etv5*^fl/fl

Figure 5. *Etv* Mutations Rescue Insulin Secretion and Granule Docking Defects Caused by COP1 Deficiency

(A) Insulin secretion from islets incubated in vitro with the stimuli indicated for 1 hr at 37°C is shown.

(B) Electron micrographs of β cells. White dotted line outlines plasma membrane. ΔCop1β; ΔEtvβ, ΔCop1β *Etv1*^fl/fl *Etv4*^ko/ko *Etv5*^fl/fl. Scale bars, 0.2 μm.

(C) Quantification of docked insulin granules. The distance from the granule center to the plasma membrane was binned into two groups. Data are presented as percentage granule density relative to cytoplasmic density (average granule density in cytoplasm equals 100%) (Gomi et al., 2005).

Analyses used mice at 3 weeks post-tamoxifen with fasting blood glucose levels between 60 and 120 mg/dl. Data are represented as mean ± SEM (*p < 0.05 and ***p < 0.0005 by unpaired Student's t test).

ΔCop1β *Etv4*^ko/ko *Etv5*^fl/fl islets (Figure 4H), perhaps reflecting compensatory mechanisms triggered by the loss of ETV4 and ETV5. Strikingly, ΔCop1β *Etv1*^fl/fl *Etv4*^ko/ko *Etv5*^fl/fl mice lacking all three ETV transcription factors in β cells did not exhibit the glucose intolerance seen in ΔCOP1β mice (Figures 4I and 4J). *Cop1*^fl/+ *Etv1*^fl/fl *Etv4*^ko/ko *Etv5*^fl/fl Pdx1.CreERT2^+ mice resembled controls in GTTs (Figure 4J), indicating that ETV deficiency does not improve glucose tolerance when COP1 is present.

Consistent with rescue of the glucose intolerance phenotype, islets from ΔCop1β *Etv1*^fl/fl *Etv4*^ko/ko *Etv5*^fl/fl mice secreted insulin

in response to KCl in vitro similar to control islets (Figure 5A). In addition, the decrease in docked insulin granules observed in the ΔCop1β pancreas was not seen in the ΔCop1β *Etv1*^fl/fl *Etv4*^ko/ko *Etv5*^fl/fl pancreas (Figures 5B and 5C). Collectively, these data indicate that elevated ETV1, ETV4, and ETV5 caused by COP1 deficiency in β cells impaired insulin secretion and drove glucose intolerance.

Identification and Functional Analysis of Pea3-Dependent Genes in β Cells

RNA sequencing of control, ΔCop1β, and ΔCop1β *Etv1*^fl/fl *Etv4*^ko/ko *Etv5*^fl/fl islets identified genes that were dysregulated in ΔCop1β islets as a result of increased ETV1, ETV4, and ETV5 (Figure 6A; GEO: GSE70788). Of the genes that were dysregulated in ΔCop1β islets, 77% approached expression levels seen in controls upon concomitant deletion of ETV1, ETV4, and ETV5 (Figure 6B; Table S1). Genetic variants associated with diabetes risk, identified from the National Human Genome Research Institute (NHGRI) GWAS catalog (Welter et al., 2014), were significantly enriched among these ETV-dependent genes (25/483 genes) (Figure 6C; Table S2). In contrast, COP1-dependent genes not rescued by ETV deletion were not significantly represented (2/170 genes). Further, given the known association between ETV5 and obesity (Welter et al., 2014), analysis of genetic variants associated with obesity showed significant representation among ETV-dependent genes (13/483 genes) (Figure 6C; Table S3).

Two ETV-dependent genes (Figures 6A and 6B; Figure S7A) stood out because of their potential involvement in granule docking: *Exocyst-6* (*Exoc6*) and *Synaptotagmin-like 3* (*Sytl3*). EXOC6 is a known component of the Exocyst complex that docks insulin granules to the plasma membrane (Saito et al., 2008; Tsuboi et al., 2005; Xie et al., 2013). SYTL3 has been shown to bind to Rab27A (Fukuda, 2013; Wang et al., 2013), a small GTPase that mediates insulin granule docking (Kasai et al., 2005). The qRT-PCR confirmed that these genes were upregulated in an ETV-dependent manner in ΔCop1β islets (Figures 6D and 6E). To determine if these genes were direct targets of ETV1, ETV4, or ETV5, we looked for potential ETV-binding motifs within their promoters. Sequences fitting the consensus ETV core binding motif G(C/A)GGA(A/T)(G/A) were identified (Figures S7C and S7D) and their deletion or mutation compromised the ability of the promoter sequences to drive ETV5-dependent expression of a luciferase reporter gene (Figures S7E and S7F). These data are consistent with *Exoc6* and *Sytl3* being direct transcriptional targets of the ETVs.

To directly determine if EXOC6 and SYTL3 impact insulin secretion, we overexpressed them in mouse insulinoma βtc6 cells that secrete insulin constitutively. In contrast to ectopic ETV5, which decreased insulin secretion from βTC6 cells, overexpression of either EXOC6 or SYTL3 alone did not result in a statistically significant reduction in insulin secretion (Figure 6F). Co-expression of EXOC6 and SYTL3, however, did cause a significant reduction in insulin secretion (Figure 6F). These results suggest that expression of *Exoc6* and *Sytl3* by ETV transcription factors is inhibitory to insulin secretion.
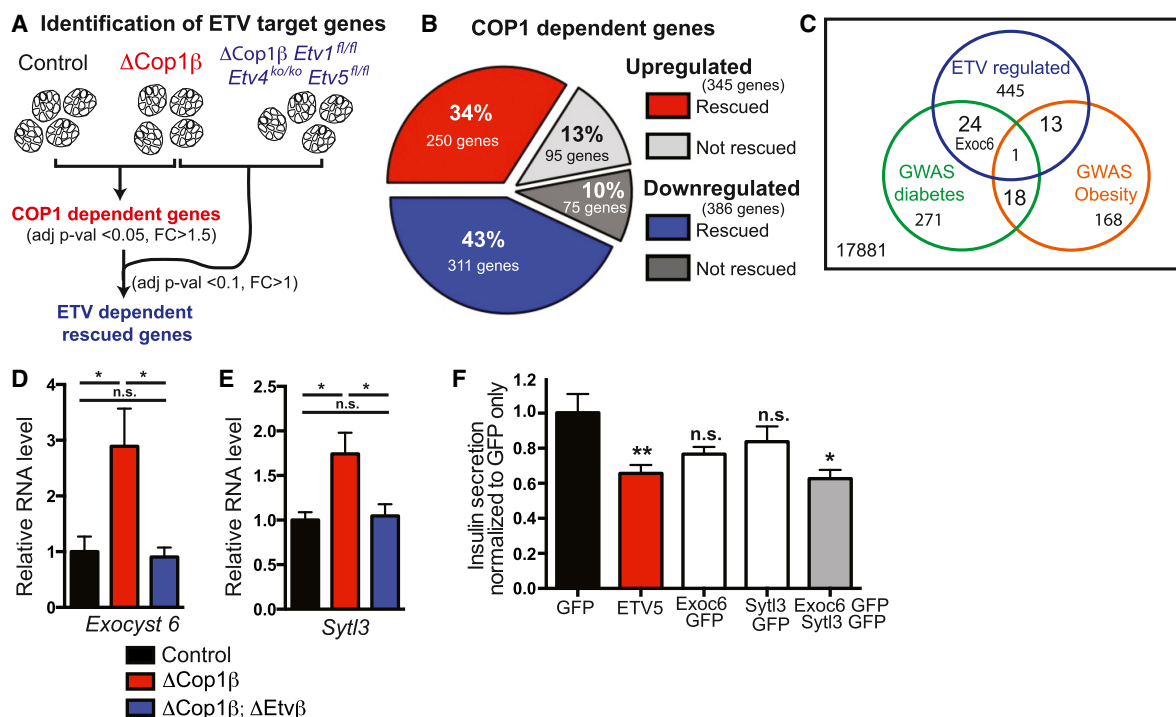
Figure 6. Expression of ETV Target Genes *Exoc6* and *Sytl3* Correlate with Decreased Insulin Secretion

(A) RNA sequencing strategy to identify ETV-dependent genes in adult ΔCop1β islets is shown.

(B) Percentages of genes dysregulated in ΔCop1β islets that were normalized in the absence of ETV1, ETV4, and ETV5 are shown.

(C) Venn diagram represents the overlap among ETV-regulated, diabetes GWAS, and obesity GWAS genes.

(D and E) Expressions of *Exoc6* (d) and *Sytl3* (e) in islets are shown.

(F) Insulin secretion from transfected βtc6 cells is shown.

Data are represented as mean ± SEM (*p < 0.05 and ***p < 0.0005 by unpaired Student's t test). Analyses used mice at 3 weeks post-tamoxifen with fasting blood glucose levels between 60 and 120 mg/dl. See also Figure S7 and Tables S1, S2, and S3.

## ETV4 Inhibits Insulin Secretion after Prolonged Glucose Stimulation

Given that a significant subset of ETV-dependent genes was enriched in diabetes-associated genes, ETV transcription factors also may function in normal glucose homeostasis. Interestingly, normal β cells expressed a lot more ETV4 protein after stimulation with the depolarizing agent potassium chloride for 20 min (Figure 7A). *Etv4* mRNA abundance was unchanged (Figure 7A), indicating that a post-translational mechanism was responsible for the increase in ETV4 protein. ERK inhibition suppressed the increase in ETV4 protein (Figure 7A), which is consistent with previous studies identifying ETS proteins as effectors of the MEK/ERK MAPK pathway (Yordy and Muise-Helmericks, 2000). To investigate whether ETV4 serves to inhibit insulin secretion after membrane depolarization, we compared the insulin secretory response of ETV4-deficient islets with that of control islets after incubation in high glucose for 16 hr (Figure 7B). Potential compensatory changes in ETV1 and ETV5 abundance due to ETV4 loss were avoided by using islets isolated from tamoxifen-treated *Etv1^fl/fl Etv4^ko/ko Etv5^fl/fl* Pdx1.CreERT2^+ (ΔETVβ) and *Etv1^fl/fl Etv4^ko/+ Etv5^fl/fl* Pdx1.CreERT2^+ (control) littermates. Consistent with the literature (Yamazaki et al., 2006), control islets exhibited attenuated GSIS after incubation in 10 mM compared to 5 mM glucose (Figure 7C, black bars). In

contrast, ΔETVβ islets showed an equivalent GSIS whether incubated in 5 or 10 mM glucose (Figure 7C, blue bars). Indeed, ΔETVβ islets exhibited increased insulin secretion in 10 mM glucose when compared to controls (Figure 7C, black versus blue bars). These results indicate that ETV4 inhibits insulin secretion after prolonged glucose stimulation (Figure 7D).

DISCUSSION

In this study, we identified a requirement for COP1, an E3 ligase that regulates the transcription factors ETV1, ETV4, and ETV5, in adult β-cell maintenance. In the absence of COP1, mice developed elevated fasting glycemia due to impaired insulin secretion. The hyperglycemia seen upon COP1 deletion was not driven by peripheral insulin resistance, but rather by impaired GSIS in β cells. The variability in hyperglycemic onset within the ΔCOP1β cohort probably represents the ability of individual mice to compensate for their impaired secretory response. Over time, similar to type 2 diabetic patients (Weir and Bonner-Weir, 2004), some animals must fail to keep up with the increased insulin secretory demand and reach thresholds of cellular exhaustion and glucose toxicity, leading to chronic hyperglycemia. Consistent with this notion, islets isolated from 10-month-old hyperglycemic ΔCOP1β animals exhibited increased endoplasmic
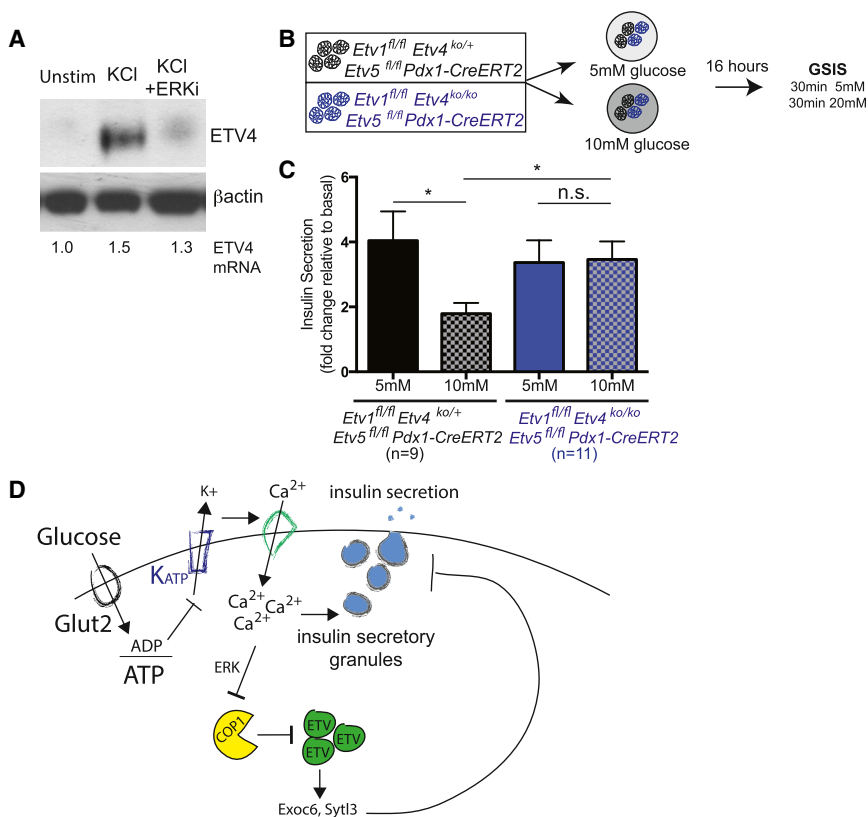
Figure 7. High Glucose-Dependent GSIS Attenuation Is Dependent on ETV4

(A) Pan-ETV immunoblot of islet lysates treated with 11.8 mM glucose/RPMI/FBS ± 30 mM KCl with or without ERK inhibitor for 20 min. ETV4 mRNA levels are indicated for each stimulation.

(B) Schematic shows the varied glucose treatment on isolated islets prior to GSIS.

(C) In vitro GSIS from islets islolated from animals 3 weeks post-tamoxifen is shown.

Data are represented as mean ± SEM (*p < 0.05 by unpaired Student's t test).

(D) Model for COP1 and ETV function during GSIS in adult β cells. Membrane depolarization during GSIS pathway activation stabilizes ETV transcription factors. Accumulation of ETV protein levels activates genes that are inhibitory to insulin granule exocytosis.

reticulum (ER) stress, which is commonly associated with glucose toxicity (Back and Kaufman, 2012; Figure S1F).

The glucose intolerance caused by COP1 deletion was a consequence of diminished GSIS. We narrowed the phenotype to abnormalities with the insulin granule pool, because membrane depolarization using KCl and arginine failed to elicit a secretory response despite normal calcium signaling. The ΔCop1β islets had a paucity of granules docked at the plasma membrane for the first phase of insulin secretion (Gaisano, 2014). Exendin-4 or activators of the incretin pathway stimulated the glucose-mediated release of ΔCop1β insulin granules, perhaps reflecting the ability of PKA to recruit new granules to the plasma membrane (Seino et al., 2011). Regardless, these data highlighted that the insulin granules in ΔCop1β islets were inherently functional for exocytosis.

Insulin secretion involves the transport, docking, and fusion of insulin granules to the plasma membrane, a process that is regulated by conserved protein families, such as Rab GTPases, and soluble *N*-ethylmaleimide-sensitive factor attachment protein receptors (SNAREs) (Wang and Thurmond, 2009). We identified two genes dysregulated upon deletion COP1, *Exoc6* and *Sytl3*, whose functions were previously uncharacterized in β cells but have been known to include interaction with components of the insulin secretory machinery. EXOC6 (also known as yeast SEC15) is part of the mammalian SEC6-SEC8 exocyst complex, which has been shown to function in insulin granule docking and secretion (Saito et al., 2008; Tsuboi et al., 2005; Xie et al., 2013). Truncations in components of this complex decrease the supply

of insulin granules close to the plasma membrane, possibly by functioning in the conversion of reserve granules to the readily releasable pool (Tsuboi et al., 2005). We found that expression of the calcium-sensitive Rab27a-binding protein *Sytl3* also was increased in ΔCop1β islets, which may further contribute to the impairment in vesicle docking (Fukuda, 2002; Fukuda et al., 2002; Kurowska et al., 2012). The small monomeric GTPase Rab27a also is required for the release and replenishment of docked granules during GSIS (Kasai et al., 2005). We hypothesize that a subset of ETV-dependent genes, including *Exoc6* and *Sytl3*, act in concert to modulate the insulin secretory defect in ΔCop1β islets. In support of this, expression of either *Exoc6* or *Sytl3* had no effect on insulin secretion, but expression of both genes significantly attenuated insulin secretion in βTC6 cells.

We identified Pea3 transcription factors as the critical COP1 substrates in pancreatic β cells. The accumulation of ETV4 and ETV5 caused the phenotypes found after deletion of COP1 in β cells. However, deletion of ETV4 and ETV5 alone was not sufficient to normalize the phenotypes seen in ΔCop1β mice because of an unexpected compensatory increase in ETV1. Consequently, it is only upon deletion of all three Pea3 family members, ETV1, ETV4, and ETV5, that phenotypes arising from COP1 deletion were fully reversed. Of the β-cell-specific ETV-dependent genes identified, there was significant enrichment of diabetes and obesity-associated genes, including *Exoc6*. ETV5 itself has been linked in GWASs to obesity and previous studies have revealed that whole-body *Etv5* knockout mice are leaner and have reduced body weight compared to control animals (Gutierrez-Aguilar et al., 2014). It would be interesting to determine if the ETV-dependent genes we identified are direct targets of ETV5 in obesity models and whether they function in regulating BMI and/or energy expenditure.

While we have uncovered a mechanism by which insulin secretion can be suppressed through the accumulation of ETV

transcription factors and their gene targets, when is this regulatory mechanism important? We believe that it represents an important feedback mechanism in β cells following sustained exposure to membrane-depolarizing secretagogues, including high potassium and high glucose. This mechanism would prevent unabated insulin release and the exhaustion of insulin reserves. Others have shown that modest but sustained exposure of β cells to elevated potassium and glucose results in a desensitization phenomenon and a dose-dependent decrement in insulin secretion (Yamazaki et al., 2006). However, the molecular mechanism underlying this phenomenon was unclear. We show that ETV4 protein abundance increased in islets cultured with potassium chloride and, consistent with a role for ETV4 in desensitization, high glucose attenuated insulin release from control islets, but not ETV4-deficient islets. This attenuation, which at late stages is classically attributed to degranulation of the β cell, may reflect an intrinsic mechanism to dampen insulin secretion to prevent cellular stress and/or insulin exhaustion (Figure 7D). In keeping with this notion, *Etv4^{ko/ko} Etv5^{fl/fl}* Pdx1.Cre animals show partial resistance to high-fat diet (data not shown), though non-β-cell effects cannot be ruled out due to the systemic deletion of ETV4. Future studies will clarify the β-cell-specific role of ETV transcription factors in high-fat diet models and other situations of increased insulin secretory demand and β-cell exhaustion.

EXPERIMENTAL PROCEDURES

Generation of Mice

Cop1^{Δ1/+}, *Cop1^{fl/fl}*, *Etv4^{ko/ko}*, *Etv5^{fl/fl}*, *Etv1^{fl/fl}*, and Pdx1.CreERT2 mice were described previously (Gu et al., 2002; Patel et al., 2003; Vitari et al., 2011; Zhang et al., 2009). CreERT2 was activated in mice by intraperitoneal injections of 100 mg/kg tamoxifen dissolved in sunflower seed oil (Sigma) for 5 consecutive days. The Genentech Institutional Animal Care and Use Committee approved all protocols.

Genotyping

Cop1 exon 1 primers 5′-GCTACCATTACCAGTTGGTCTGGTGTC-3′, 5′-CCAACCCCACAAGTTCAGGGAT-3′, and 5′-CTGCATCATGTTGTGTGATTGCAT-3′ yield 873-bp wild-type and 532-bp knockout DNA fragments. *Cop1* exon 3 primers 5′-CATTGAAATGATAATTGCAGATTTGGTC-3′, 5′-CACCACCCTGCCAGATCTTAAATATAGAT-3′, and 5′-CAAACCTGTCACAAAATACTATTGTGCTCTC-3′ yield 686-bp wild-type, 753-bp floxed, and 452-bp knockout DNA fragments. *Cre*-specific primers 5′-GCTAAACATGCTTCATCGTCGGTC-3′ and 5′-CCAGACCAGGCCAGGTATCTCTG-3′ amplified a 582-bp fragment.

Histology and Immunohistochemistry

Whole pancreas was fixed in 4% paraformaldehyde for immunofluorescence staining or 20% Formalin for staining with H&E. β-galactosidase enzymatic activity was revealed by incubating 10-μm pancreatic sections with 0.5 mg/ml 5-bromo-4-chloro-3-indolyl-β-d-galactopyranoside (Sigma B4252) overnight at 37°C. Sections were counterstained with Nuclear Fast Red (ENG Scientific 9040). When combined with immunofluorescence staining, sections were blocked with 10% normal rabbit serum and 10% normal goat serum for 30 min, and then stained with primary antibodies for 1 hr at room temperature. Slides were washed three times for 5 min each then incubated for 1 hr with Alexa-Fluor conjugated secondary antibodies (Jackson Laboratory) at room temperature. Slides were mounted with Prolong Gold (Invitrogen P36934). Imaging was performed using the Nuance Multi-spectral Imaging System (Caliper Life Sciences).

COP1 immunohistochemistry was performed on a Dako automated staining platform. Heat-induced epitope retrieval (Dako) was used for both glucagon and COP1 immunohistochemistry. Biotinylated goat anti-guinea pig IgG and goat anti-rabbit IgG were used for detection of anti-insulin and anti-glucagon antibodies in combination with ABC peroxidase Elite detection (Vector Laboratories) and DAB chromogen. Biotinylated goat anti-hamster followed by Streptavidin-horseradish peroxidase with tyramide signal amplification (PerkinElmer) and DAB chromogen were used to detect anti-COP1 antibodies. All sections were counterstained with Mayer's hematoxylin. Primary antibodies used were as follows: guinea pig anti-insulin (Dako A056401-2, 5.5 μg/ml), rabbit anti-glucagon (Cell Signaling Technology 2760, 0.04 μg/ml), mouse pro-insulin (Developmental Studies Hybridoma Bank [DSHB] GS-9A8), and hamster monoclonal anti-COP1 antibody (Genentech IDIO.10.4.4.1, 0.12 μg/ml).

In Vivo GTTs and GSIS Assays

Mice fasted 15–18 hr were injected intraperitoneally with 2 mg glucose/g body weight or given 1 mg glucose/g body weight orally. Blood samples were taken by tail vein nick for glucose measurement (FreeStyle Lite glucometer) and serum collection. Treatment with Exendin-4 (5 μg/kg body weight) was conducted 15 min prior to injection of 2 mg/kg glucose. Serum insulin was measured by ELISA (Alpco).

Hyperglycemic Clamping

Hyperglycemic clamping of mice was conducted at the Vanderbilt University Mouse Metabolic Phenotyping Center as previously described (Berglund et al., 2008).

Islet Harvest and Secretogogue Assays

Islets were harvested from mice 3 weeks post-tamoxifen by collagenase digestion, histopaque density centrifugation (Sigma 11191), and hand picking (Kaihara et al., 2013). After overnight recovery in RPMI medium containing 11.8 mM glucose, 10% FBS, 50 μg/ml penicillin, and 50 μg/ml streptomycin, ten islets per mouse were transferred into Kreb's buffer containing 2.8 mM glucose for 1 hr to measure basal insulin secretion. After supernatant removal, secretogogues (16.8 mM glucose, 30 mM KCl in 2.8 mM glucose or 20 mM arginine in 2.8 mM glucose) in Kreb's buffer were added to the islets for 1 hr. For experiments requiring activator pretreatment, 100 nM Exendin-4 (Sigma e7144), 10 μM Forskolin (R&D Systems 1099), 10 μM Epac activator 8-pCPT-2-O-Me-cAMP-AM (R&D Systems 4853), and/or 10 μM PKA activator *N^6*-Benzoyladenosine-3′,5′-cyclic monophosphate (R&D Systems 5255) was added 15 min prior to KCl stimulation. Insulin in the supernatants was measured using Meso Scale Discovery (MSD) standard insulin assay. Results are presented as total insulin secreted after normalization to basal secretion in 2.8 mM glucose. For measurements of insulin content, islets were lysed in radioimmunoprecipitation assay (RIPA) buffer and insulin content was measured using the MSD standard insulin assay. DNA and protein content in the same lysates were measured to account for differences in islet size.

Islet Perfusion Assays

Islets from normoglycemic control and ΔCop1β mice were harvested 3 weeks post-tamoxifen treatment. Harvested islets were incubated overnight in RPMI containing 11.8 mM glucose, 10% FBS, 50 U/ml penicillin, and 50 μg/ml streptomycin and then placed in a perifusion chamber as previously described (Kaihara et al., 2013). Flow rate of fluid input (2.8 mM glucose, 16.6 mM glucose, or 30 mM KCl in Kreb's buffer) was 1 ml/min and fractions were collected every minute. Graph represents three perifusions from three different mice per group.

Calcium Imaging

As previously described (Kaihara et al., 2013), isolated islets were incubated with 5 μM fura-2-AM (Invitrogen) in 2 mM glucose-Kreb's buffer for 30 min. Image measurements were acquired at 10-s intervals and data were expressed as the fold change in the $A_{340\ nm}/A_{380\ nm}$ ratio normalized to basal 2.8-mM glucose readings.

Electron Microscopy and Morphometric Measurements

Samples were fixed in 1/2 Karnovsky's fixative (2% paraformaldehyde and 2.5% glutaraldehyde in 0.1 M sodium cacodylate buffer [pH 7.2]), post-fixed in 1% aqueous osmium textroxide, and dehydrated through a series of ethanol washes followed by two propylene oxide washes. Samples were embedded in Eponate 12 (Ted Pella) and cured at 65°C overnight. Semi-thin (300-nm) and

ultrathin (80-nm) sections were obtained with an Ultracut microtome (Leica). Semi-thin sections were stained with toluidine blue and examined by bright-field microscopy to identify islets. Once islets were identified, parallel ultrathin sections were prepared, counterstained with 1% uranyl acetate and 0.2% lead citrate, and examined in a JEOL JEM-1400 transmission electron microscope (TEM) at 120 kV. Images were captured with a GATAN Ultrascan 1000 CCD camera. For immunogold labeling, samples were fixed in 4% paraformaldehyde and 0.2% glutaraldehyde in 0.1 M phosphate buffer (pH 7.2). Samples were washed, dehydrated, and infiltrated with LR White resin (London Resin). Sample blocks were cured at 55°C overnight. Ultrathin sections were labeled with a polyclonal anti-insulin antibody (Dako), followed by biotinylated donkey anti-guinea pig antibody (Jackson ImmunoResearch Laboratories) and streptavidin conjugated with 15 nm colloidal gold particles (Electron Microscopy Sciences). Labeled sections were counterstained with 2% uranyl acetate and imaged as described above.

Morphometry

Dense core vesicle size distribution bar graphs are presented as dense core vesicle size (circumference in pixels using ImageJ software) as a function of percentage total vesicles. Circumferences of 80 vesicles were measured from two animals per genotype.

Docked insulin granules were measured as described previously (Gomi et al., 2005). Briefly, the distance from granule centers to the plasma membrane was measured and then binned into two groups (0–100 nm and 100–300 nm). The data are represented as percentage granule density (granules/area) relative to cytoplasmic density (granule density in cytoplasm equals 100%).

qRT-PCR

Total cellular RNA was prepared using an RNeasy kit (QIAGEN) with on-column DNase treatment. RT-PCR reactions were performed in 384-well plates on a 7900HT Fast Real-Time PCR System (Applied Biosystems). Taqman gene expression assays (Applied Biosystems) were as follows: *Pdx1*, mM00435565_m1; *Nkx6.1*, Mm00454961_m1; *Neurod1*, Mm01280117_m1; *Ngn3*, Mm00437606_s1; *Sox9*, Mm00448840_m1; *Hes1*, Mm01342805_m1; *Nanog*, Mm02384862_g1; *Oct4*, Mm03053917_g1; *Sox2,* Mm03053810_s1; *Ins1*, Mm01950294_s1; *Ins2*, Mm00731595_gH; *Exoc6*, Mm00558419_m1; and *Sytl3*, Mm00473333_m1.

Western Blots

Antibodies recognized β-actin (Novus Biologicals NB600-501); COP1 (Genentech 28A4); ETV1, 4, or 5 (Genentech 20H5); ETV1 (Genentech 13G11); and Exoc6 (Novus NBP1-85031). The islets (100) were lysed in 50 μl RIPA buffer with 10% SDS, phosSTOP phosphatase, and protease inhibitors (Roche); 15 μl denatured lysate was run per sample.

Insulin Secretion in βTC6 Cells

Insulin secretion was measured 48 hr after βtc6 cells were transfected using Lipofectamine 3000 (Life Technologies). Total secreted insulin was measured from supernatant collected after a 1-hr incubation in fresh medium (DMEM, 15% FBS, 50 U/ml penicillin, and 50 μg/ml streptomycin).

RNA Sequencing

RNA was extracted from adult islets using RNeasy kits (QIAGEN) with on-column DNase treatment. RNA (500 ng–1 μg) was submitted for analysis using the Illumina HiSeq 2500 platform. Sequencing reads were aligned to the mouse genome (NCBI37) with RefSeq gene models (RefSeq version 53, downloaded on June 16, 2012) using GSNAP (version 2013-10-10) and the following parameters: -M 2 -n 10 -B 2 -i 1 -N 1 -w 200000 -E 1–pairmax-rna = 200000–clipoverlap. Gene expression levels were computed by summing the number of reads mapping to exons of RefSeq genes. Counts were normalized using size factors (as described by DESeq2) to account for library size variation. Differential expression between groups of samples was computed on the normalized counts using the R DESeq2 package. *Cop1*-dependent genes were identified as genes differentially expressed between the control and ΔCop1β islets (adjust p < 0.05, fold change > 1.5). From this list, ETV-dependent rescued genes were identified as differentially expressed genes (in the same direction) between ΔCop1β and ΔCop1β; ΔEtvβ islets (adjusted p < 0.1).

Diabetes and Obesity GWAS Analysis

GWAS data were obtained from the NHGRI GWAS catalog (Welter et al., 2014; downloaded on December 19, 2014) using the following search terms: diabetes, obesity, and BMI. A total of 468 diabetes- and 322 obesity-associated SNPs were identified. Genes reported or mapped by the catalog to be associated with these SNPs were then mapped to their mouse orthologs using the Ensembl Biomart orthology mapping (Biomart version 77, October 2014). The overlap between ETV-dependent genes and the GWAS diabetes/obesity gene sets was evaluated using a permutation test.

ACCESSION NUMBERS

The accession number for the RNA sequencing reported in this paper is GEO: GSE70788.

SUPPLEMENTAL INFORMATION

Supplemental Information includes seven figures and three tables and can be found with this article online at http://dx.doi.org/10.1016/j.cell.2015.10.076.

REFERENCES

Back, S.H., and Kaufman, R.J. (2012). Endoplasmic reticulum stress and type 2 diabetes. Annu. Rev. Biochem. *81*, 767–793.

Berglund, E.D., Li, C.Y., Poffenberger, G., Ayala, J.E., Fueger, P.T., Willis, S.E., Jewell, M.M., Powers, A.C., and Wasserman, D.H. (2008). Glucose metabolism in vivo in four commonly used inbred mouse strains. Diabetes *57*, 1790–1799.

Dentin, R., Liu, Y., Koo, S.H., Hedrick, S., Vargas, T., Heredia, J., Yates, J., 3rd, and Montminy, M. (2007). Insulin modulates gluconeogenesis by inhibition of the coactivator TORC2. Nature *449*, 366–369.

Drucker, D.J., and Nauck, M.A. (2006). The incretin system: glucagon-like peptide-1 receptor agonists and dipeptidyl peptidase-4 inhibitors in type 2 diabetes. Lancet *368*, 1696–1705.

Eizirik, D.L., Korbutt, G.S., and Hellerström, C. (1992). Prolonged exposure of human pancreatic islets to high glucose concentrations in vitro impairs the beta-cell function. J. Clin. Invest. *90*, 1263–1268.

Fukuda, M. (2002). The C2A domain of synaptotagmin-like protein 3 (Slp3) is an atypical calcium-dependent phospholipid-binding machine: comparison with the C2A domain of synaptotagmin I. Biochem. J. *366*, 681–687.

Fukuda, M. (2013). Rab27 effectors, pleiotropic regulators in secretory pathways. Traffic *14*, 949–963.

Fukuda, M., Kanno, E., Saegusa, C., Ogata, Y., and Kuroda, T.S. (2002). Slp4-a/granuphilin-a regulates dense-core vesicle exocytosis in PC12 cells. J. Biol. Chem. *277*, 39673–39678.

Gaisano, H.Y. (2014). Here come the newcomer granules, better late than never. Trends Endocrinol. Metab. *25*, 381–388.

Gomi, H., Mizutani, S., Kasai, K., Itohara, S., and Izumi, T. (2005). Granuphilin molecularly docks insulin granules to the fusion machinery. J. Cell Biol. 171, 99–109.

Gu, G., Dubauskaite, J., and Melton, D.A. (2002). Direct evidence for the pancreatic lineage: NGN3+ cells are islet progenitors and are distinct from duct progenitors. Development 129, 2447–2457.

Gutierrez-Aguilar, R., Kim, D.H., Casimir, M., Dai, X.Q., Pfluger, P.T., Park, J., Haller, A., Donelan, E., Park, J., D'Alessio, D., et al. (2014). The role of the transcription factor ETV5 in insulin exocytosis. Diabetologia 57, 383–391.

Kahn, B.B. (1998). Type 2 diabetes: when insulin secretion fails to compensate for insulin resistance. Cell 92, 593–596.

Kahn, S.E. (2001). Clinical review 135: The importance of beta-cell failure in the development and progression of type 2 diabetes. J. Clin. Endocrinol. Metab. 86, 4047–4058.

Kaihara, K.A., Dickson, L.M., Jacobson, D.A., Tamarina, N., Roe, M.W., Philipson, L.H., and Wicksteed, B. (2013). β-Cell-specific protein kinase A activation enhances the efficiency of glucose control by increasing acute-phase insulin secretion. Diabetes 62, 1527–1536.

Kasai, K., Ohara-Imaizumi, M., Takahashi, N., Mizutani, S., Zhao, S., Kikuta, T., Kasai, H., Nagamatsu, S., Gomi, H., and Izumi, T. (2005). Rab27a mediates the tight docking of insulin granules onto the plasma membrane during glucose stimulation. J. Clin. Invest. 115, 388–396.

Kitamura, T. (2013). The role of FOXO1 in β-cell failure and type 2 diabetes mellitus. Nat. Rev. Endocrinol. 9, 615–623.

Kurowska, M., Goudin, N., Nehme, N.T., Court, M., Garin, J., Fischer, A., de Saint Basile, G., and Ménasché, G. (2012). Terminal transport of lytic granules to the immune synapse is mediated by the kinesin-1/Slp3/Rab27a complex. Blood 119, 3879–3889.

Lau, O.S., and Deng, X.W. (2012). The photomorphogenic repressors COP1 and DET1: 20 years later. Trends Plant Sci. 17, 584–593.

Lu, B.C., Cebrian, C., Chi, X., Kuure, S., Kuo, R., Bates, C.M., Arber, S., Hassell, J., MacNeil, L., Hoshi, M., et al. (2009). Etv4 and Etv5 are required downstream of GDNF and Ret for kidney branching morphogenesis. Nat. Genet. 41, 1295–1302.

Ma, L., Gao, Y., Qu, L., Chen, Z., Li, J., Zhao, H., and Deng, X.W. (2002). Genomic evidence for COP1 as a repressor of light-regulated gene expression and development in Arabidopsis. Plant Cell 14, 2383–2398.

Magnuson, M.A., and Osipovich, A.B. (2013). Pancreas-specific Cre driver lines and considerations for their prudent use. Cell Metab. 18, 9–20.

Mao, J., McGlinn, E., Huang, P., Tabin, C.J., and McMahon, A.P. (2009). Fgf-dependent Etv4/5 activity is required for posterior restriction of Sonic Hedgehog and promoting outgrowth of the vertebrate limb. Dev. Cell 16, 600–606.

Marine, J.C. (2012). Spotlight on the role of COP1 in tumorigenesis. Nat. Rev. Cancer 12, 455–464.

Migliorini, D., Bogaerts, S., Defever, D., Vyas, R., Denecker, G., Radaelli, E., Zwolinska, A., Depaepe, V., Hochepied, T., Skarnes, W.C., and Marine, J.C. (2011). Cop1 constitutively regulates c-Jun protein stability and functions as a tumor suppressor in mice. J. Clin. Invest. 121, 1329–1343.

Orci, L., Ravazzola, M., Amherdt, M., Madsen, O., Vassalli, J.D., and Perrelet, A. (1985). Direct identification of prohormone conversion site in insulin-secreting cells. Cell 42, 671–681.

Patel, T.D., Kramer, I., Kucera, J., Niederkofler, V., Jessell, T.M., Arber, S., and Snider, W.D. (2003). Peripheral NT3 signaling is required for ETS protein expression and central patterning of proprioceptive sensory afferents. Neuron 38, 403–416.

Prentki, M., and Nolan, C.J. (2006). Islet beta cell failure in type 2 diabetes. J. Clin. Invest. 116, 1802–1812.

Qi, L., Heredia, J.E., Altarejos, J.Y., Screaton, R., Goebel, N., Niessen, S., Macleod, I.X., Liew, C.W., Kulkarni, R.N., Bain, J., et al. (2006). TRB3 links the E3 ubiquitin ligase COP1 to lipid metabolism. Science 312, 1763–1766.

Rorsman, P., and Braun, M. (2013). Regulation of insulin secretion in human pancreatic islets. Annu. Rev. Physiol. 75, 155–179.

Rorsman, P., and Renström, E. (2003). Insulin granule dynamics in pancreatic beta cells. Diabetologia 46, 1029–1045.

Rustenbeck, I., Wienbergen, A., Bleck, C., and Jörns, A. (2004). Desensitization of insulin secretion by depolarizing insulin secretagogues. Diabetes 53 (Suppl 3), S140–S150.

Saito, T., Shibasaki, T., and Seino, S. (2008). Involvement of Exoc3l, a protein structurally related to the exocyst subunit Sec6, in insulin secretion. Biomed. Res. 29, 85–91.

Seino, S., and Shibasaki, T. (2005). PKA-dependent and PKA-independent pathways for cAMP-regulated exocytosis. Physiol. Rev. 85, 1303–1342.

Seino, S., Shibasaki, T., and Minami, K. (2011). Dynamics of insulin secretion and the clinical implications for obesity and diabetes. J. Clin. Invest. 121, 2118–2125.

Song, W.J., Seshadri, M., Ashraf, U., Mdluli, T., Mondal, P., Keil, M., Azevedo, M., Kirschner, L.S., Stratakis, C.A., and Hussain, M.A. (2011). Snapin mediates incretin action and augments glucose-dependent insulin secretion. Cell Metab. 13, 308–319.

Talchai, C., Xuan, S., Lin, H.V., Sussel, L., and Accili, D. (2012). Pancreatic β cell dedifferentiation as a mechanism of diabetic β cell failure. Cell 150, 1223–1234.

Tsuboi, T., Ravier, M.A., Xie, H., Ewart, M.A., Gould, G.W., Baldwin, S.A., and Rutter, G.A. (2005). Mammalian exocyst complex is required for the docking step of insulin vesicle exocytosis. J. Biol. Chem. 280, 25565–25570.

Vitari, A.C., Leong, K.G., Newton, K., Yee, C., O'Rourke, K., Liu, J., Phu, L., Vij, R., Ferrando, R., Couto, S.S., et al. (2011). COP1 is a tumour suppressor that causes degradation of ETS transcription factors. Nature 474, 403–406.

Wang, Z., and Thurmond, D.C. (2009). Mechanisms of biphasic insulin-granule exocytosis - roles of the cytoskeleton, small GTPases and SNARE proteins. J. Cell Sci. 122, 893–903.

Wang, H., Ishizaki, R., Xu, J., Kasai, K., Kobayashi, E., Gomi, H., and Izumi, T. (2013). The Rab27a effector exophilin7 promotes fusion of secretory granules that have not been docked to the plasma membrane. Mol. Biol. Cell 24, 319–330.

Weir, G.C., and Bonner-Weir, S. (2004). Five stages of evolving beta-cell dysfunction during progression to diabetes. Diabetes 53 (Suppl 3), S16–S21.

Welter, D., MacArthur, J., Morales, J., Burdett, T., Hall, P., Junkins, H., Klemm, A., Flicek, P., Manolio, T., Hindorff, L., and Parkinson, H. (2014). The NHGRI GWAS Catalog, a curated resource of SNP-trait associations. Nucleic Acids Res. 42, D1001–D1006.

Xie, L., Zhu, D., Kang, Y., Liang, T., He, Y., and Gaisano, H.Y. (2013). Exocyst sec5 regulates exocytosis of newcomer insulin granules underlying biphasic insulin secretion. PLoS ONE 8, e67561.

Yamazaki, H., Zawalich, K.C., and Zawalich, W.S. (2006). Desensitization of the pancreatic beta-cell: effects of sustained physiological hyperglycemia and potassium. Am. J. Physiol. Endocrinol. Metab. 291, H1381–H1387.

Yordy, J.S., and Muise-Helmericks, R.C. (2000). Signal transduction and the Ets family of transcription factors. Oncogene 19, 6503–6513.

Zhang, Z., Verheyden, J.M., Hassell, J.A., and Sun, X. (2009). FGF-regulated Etv genes are essential for repressing Shh expression in mouse limb buds. Dev. Cell 16, 607–613.